Electronic Supplementary Material (ESI) for Lab on a Chip.
This journal is © The Royal Society of Chemistry 2018

Supporting information

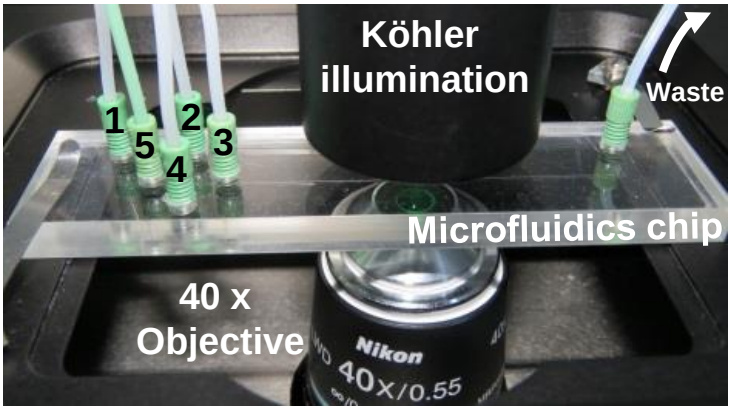

Supplemental Figure S1. Details of the microfluidics chip. The PMMA chip with a channel height of 50 µm, a width of 500 µm and a total length of 5,000 µm consists of four sheath inlets (indicated as 1 - 4) to form a two-dimensional sheath flow around the sample which enters the channel through inlet 5.

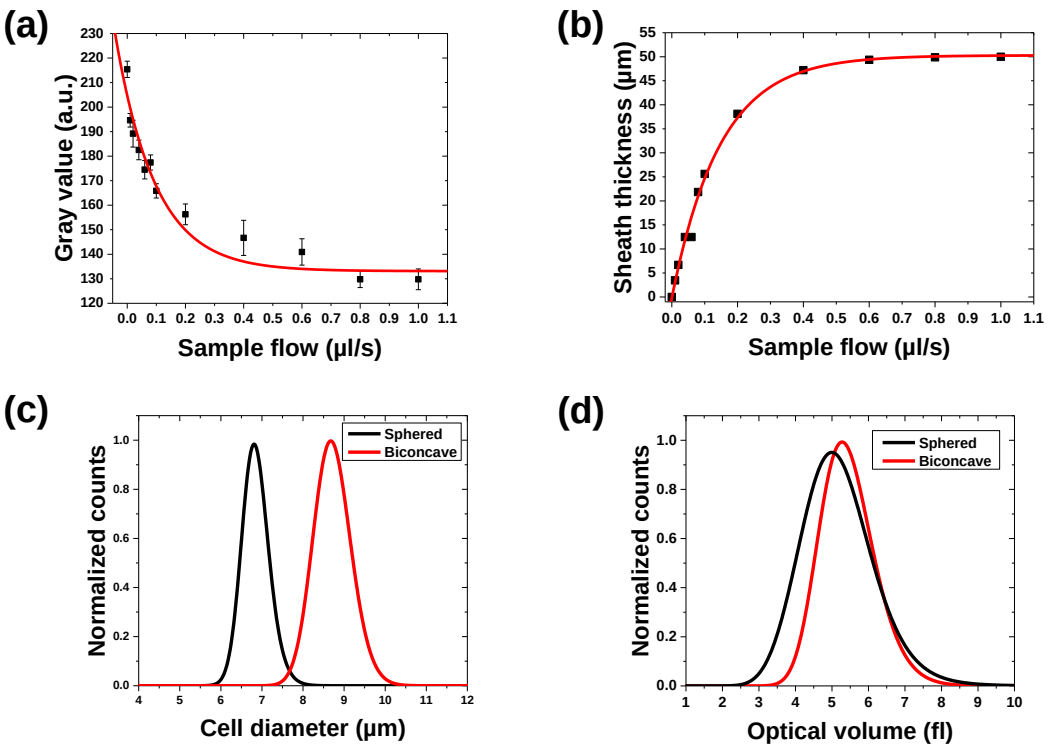

Supplemental Figure S2. Measurement of sample flow thickness and diameter and volume comparison of sphered and biconcave erythrocytes. (a) 0.1 M methylene blue in autoMACS® Rinsing Solution (Milteny Bitoec) was used to examine the sample stream height at different sample flow conditions (1 - 0 µl/s) using a Leica DM 2500 M microscope with a Baumer HXG20 camera. Two-dimensional sheath flow conditions remained constant (see Methods section). The gray value for each sample flow condition was measured at three different positions inside the channel using ImageJ. For each flow conditions, three measurements were performed. (b) Calculated sample sheath thickness in µm corresponding to measured gray values shown in (a). (c) Diameter comparison of sphered and biconcave erythrocytes measured by DHM. Mean diameter values: 6.84 ± 0.07 µm (sphered erythrocytes), 8.71 ± 0.06 µm (biconcave erythrocytes). The average distribution of five measured samples is displayed. (d) Average volume comparison of five samples with sphered and biconcave erythrocytes measured by DHM. Mean optical volume values: 5.20 ± 0.13 fl (sphered

erythrocytes), 5.40 ± 0.09 fl (biconcave erythrocytes). The similar volume distributions confirm isovolumetric sphering by the ADVIA®120 RBC/PLT sphering buffer.

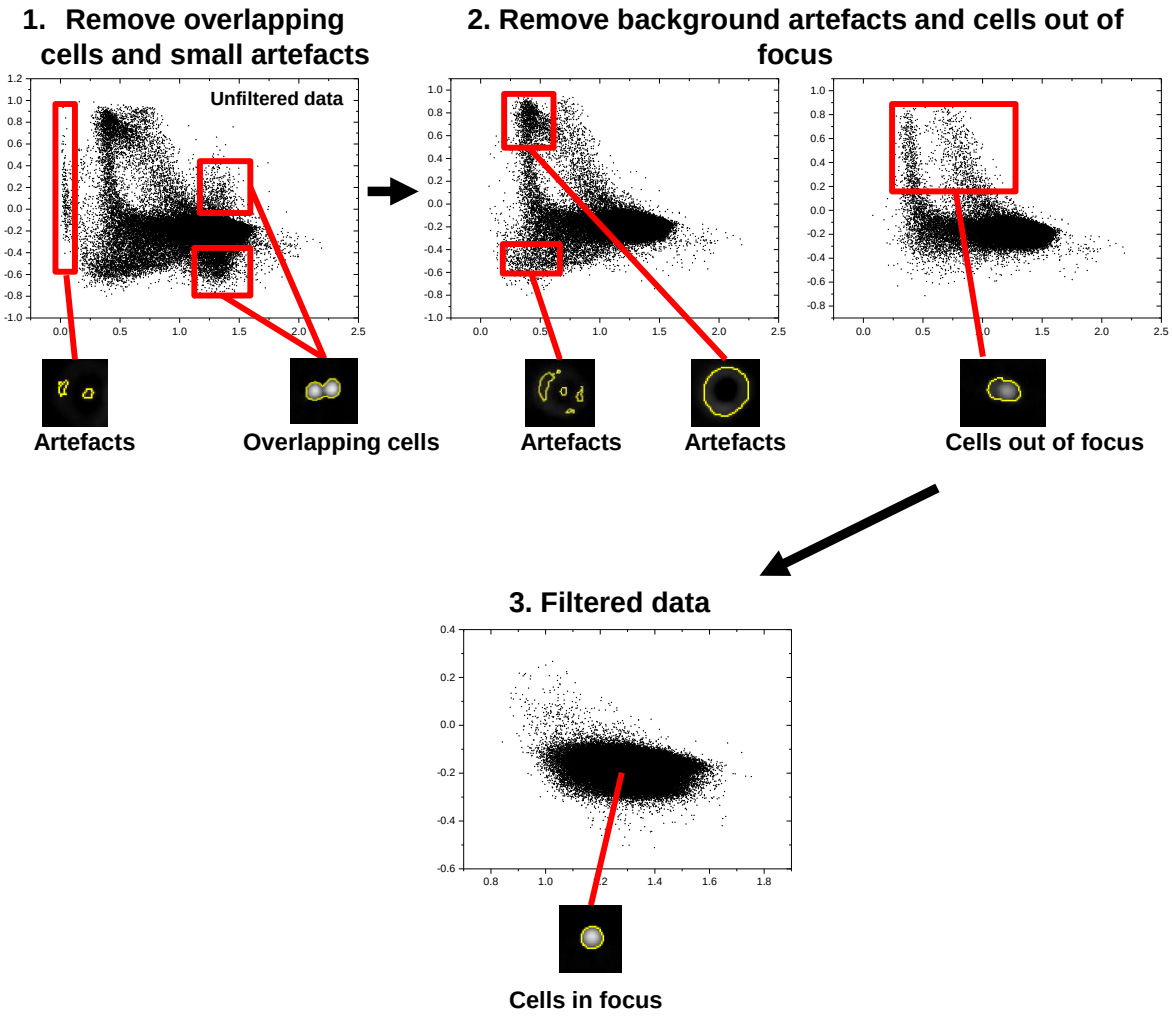

Supplemental Figure S3. Filter strategy to remove overlapping cells, artefacts and cells out of focus (~ 23 % of total count). First, overlapping cells and small artefacts were removed by thresholding of the parameter cell area (~ 10 % of all segmented objects). Second, background artefacts were removed by thresholding of the parameters aspect ratio, radius variance and optical height minimum (~ 3 % of all segmented objects). Cells out of focus were removed by thresholding of the parameters optical height mean, sphericity and

homogeneity (~ 10 % of all segmented objects) (see Supplemental Table S1 for description of parameters). Parameters biconcavity and optical height variance are plotted.

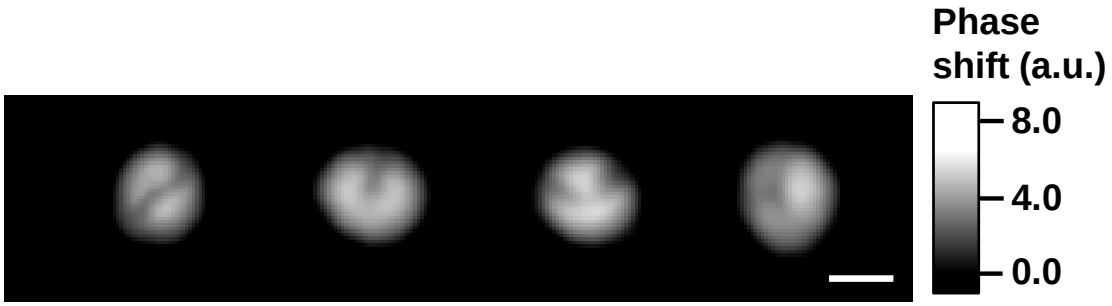

Supplemental Figure S4. Reconstructed phase images of *P. falciparum* ring stage infected sphered erythrocytes in random orientations. Infections at the ring stage can be detected independently from cellular rotation induced by microfluidics flow. Single- and double-infected erythrocytes are displayed. Scale bar is 5 µm.

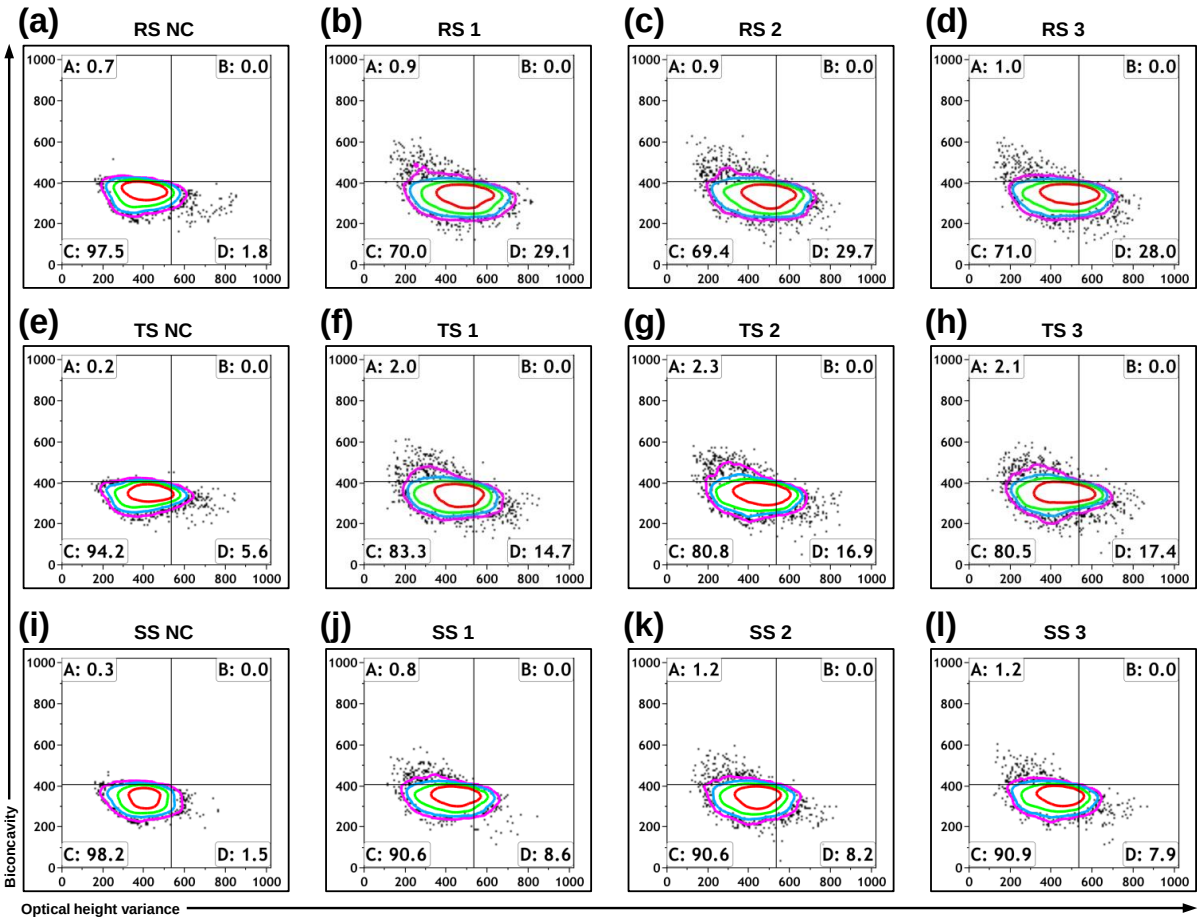

Supplemental Figure S5. Overview of analyzed *P. falciparum* samples. Synchronized samples were analyzed for (a)-(d) ring stage (RS), (e)-(h) trophozoite stage (TS), and (i)-(l) schizont stage (SS) pathogens with respective negative controls (NCs). Cells in the TS stage revealed significantly higher percentage biconcavity in quadrant A than cells in RS and SS. A significant decrease in the optical height variance from RS to SS in quadrant D was observed. Parasitemia of infected samples was > 5 %. Contour plots with optical height variance and biconcavity are plotted with outliers.

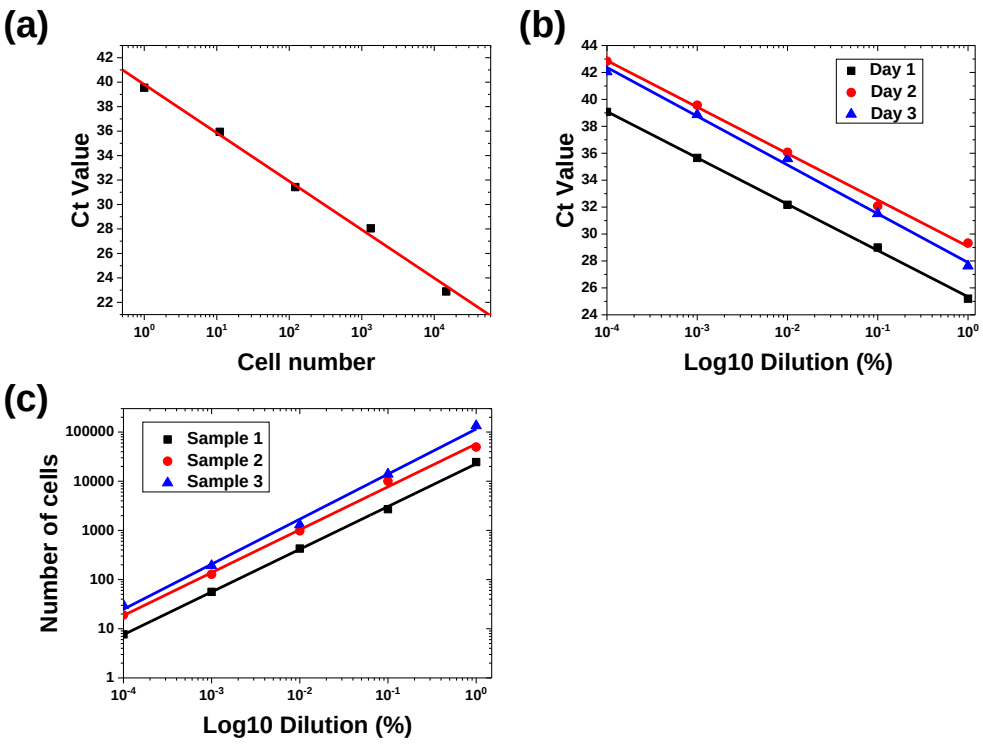

Supplemental Figure S6. Determination of the dilution accuracy by qPCR for detection limit experiments. (a) Ct values of measured standard curve. (b) Measured Ct values for parasitemia of 1, 0.1, 0.01, 0.001 and 0.0001 %. (c) Number of cells determined by alignment with measured standard curve. The observed variation in cell numbers for each measurement is related to pipetting errors.

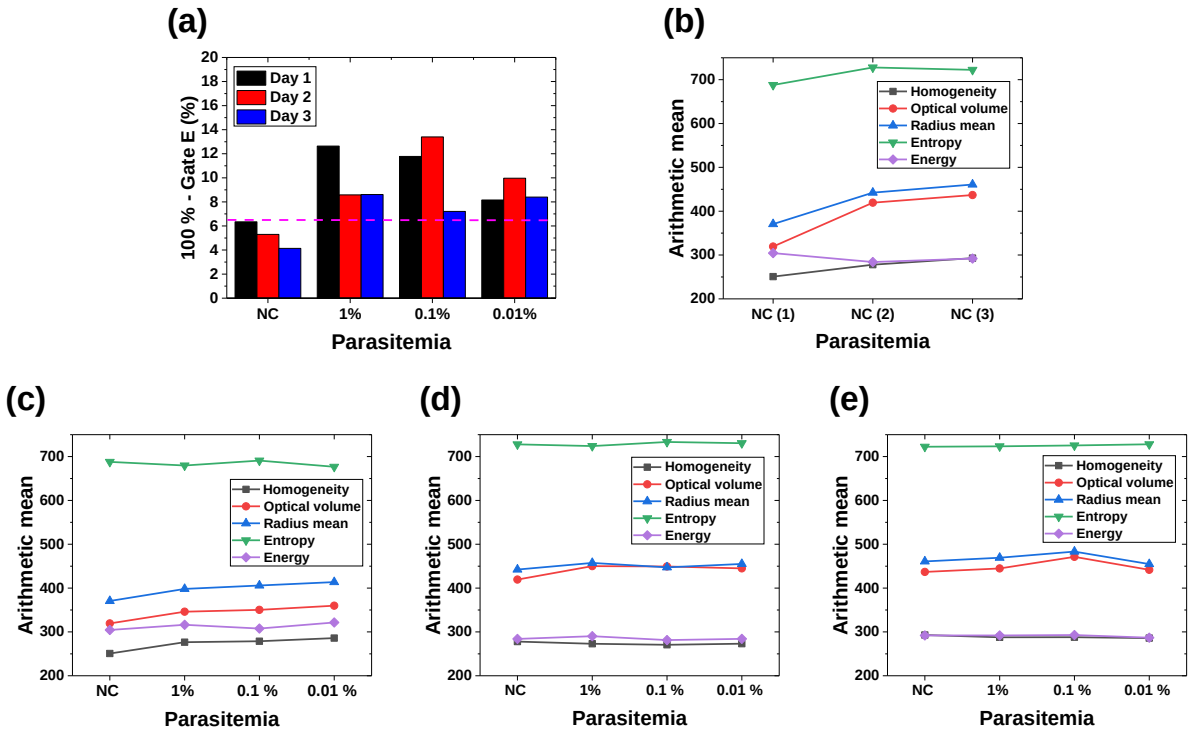

Supplemental Figure S7. Comparison of analyzed samples for detection limit experiments. (a) All measured samples with parasitemias of 1, 0.1 and 0.01 % are above the infection threshold indicated by the dashed magenta line. (b) Comparison of the parameters homogeneity, optical volume, radius mean, entropy and energy of negative controls measured at day 1 (NC (1)), day 2 (NC (2)) and day 3 (NC (3)). Note, donor blood differed between samples of day 1-3. Mean values vary between negative controls of different days. (c)-(e) Comparison of the parameters homogeneity, optical volume, radius mean, entropy and energy of measured samples at day 1 ((c)), day 2 ((d)) and day 3 ((e)). Mean values are similar within, but vary between the individual days.

Supplemental Table S1. List, description and calculation of morphological parameters.

Parameter	Unit	Description
Cell Area	µm^2	Area contained by cell contour
Perimeter	µm	Cell contour perimeter
Width	µm	Width of rotated bounding rectangle with minimum area
Height	µm	Height of rotated bounding rectangle with minimum area
Aspect ratio	a. u.	max (Width,Height) /min (Width,Height)
Circularity	a. u. (0 - 1)	The circularity of the cell contour. Calculated by 4π* cellArea / perimeter^2. Circularity of a perfect circle is 1.
Radius mean	µm	The mean distance between the centroid of the contour and each contour support point
Radius variance	a. u.	The variance of the distance between the centroid of the contour and each contour support point
Solidity	a. u.	Ratio of contour area to its convex hull area
Equivalent Diameter	µm	The diameter of the circle whose area is same as the contour area
Optical volume	µm^3	The overall optical volume is the sum of all pixel volumes inside the contour
Optical height maximum	a. u.	The maximum phase value inside the contour
Optical height minimum	a. u.	The minimum phase value inside the contour
Optical height mean	a. u.	The mean phase value inside the contour
Optical height variance	a. u.	The phase value variance inside the contour
Biconcavity	a. u. (-1 - 1)	A measurement for a biconcave shape of the cell. Describes the correlation of phase values on a horizontal and vertical cut in the middle of the cell contour to a idealized biconcave cell modelled by $-4x^4 + 4x^2 + 0{,}5$ is calculated.
Sphericity	a. u. (-1 - 1)	A measurement for a spherical shape of the cell. Describes the correlation of phase values on a horizontal and vertical cut in the middle of the cell contour to a idealized spherical cell modelled by $-x^2 + 1$ is calculated.
Mass Center shift	a. u.	Euclidian distance between geometric centroid and mass centroid
Contrast	a. u.	Intensity contrast between a pixel and its neighbor based on GLCM of phase values converted to 6bit grayscale image for the pixels inside cell contour.
Dissimilarity	a. u.	Dissimilarity measure based on GLCM of phase values converted to 6bit grayscale image for the pixels inside cell contour.
Homogenity	a. u.	Homogenity measure based on GLCM of phase values converted to 6bit grayscale image for the pixels inside cell contour.
Energy	a. u.	Energy measure (sum of squared elements) based on GLCM of phase values converted to 6bit grayscale image for the pixels inside cell contour.
Entropy	a. u.	Entropy measure based on GLCM of phase values converted to 6bit grayscale image for the pixels inside cell contour.

Supplemental Table S2. Overview of acquired frames, cell number, acquisition time, analysis time, and raw data size for detection limit experiments.

Parasitemia (%)	Negative control	1	0.1	0.01	0.001 (only qPCR)	0.0001 (only qPCR)
Number of frames	30.000	30.000	60.000	300.000	-	-
Number of cells						
Sample 1	150,614	188,408	358,417	1,104,275	-	-
Sample 2	557,693	399,151	859,238	2,741,902	-	-
Sample 3	305,554	194,321	365,370	1,644,954	-	-
Acquisition time (min)	4.74	4.74	9.48	47.4	-	-
Analysis time (min)	1.5	1.5	3.0	15.0	-	-
Raw data size (GB)	90	90	180	900	-	-

Supplemental Table S3. Erythrocyte sphering efficiency of the ADVIA® RBC/PLT buffer.

Data Set	Total cell number	Sphered cells	Biconcave cells	Sphered cells (%)	Biconcave cells (%)
1	1320	1154	166	87.4	12.6
2	1126	1006	120	89.3	10.7
3	1044	905	139	86.7	13.3
4	1147	1002	145	87.4	12.6
5	1389	1293	96	93.1	6.9
6	1486	1323	163	89.0	11.0
7	1170	1045	125	89.3	10.7
8	1026	998	28	97.3	2.7
9	1270	1052	218	82.8	17.2
10	1213	1140	73	94.0	6.0
Mean ± Std. Dev.		1048.5 ± 127.7	132.0 ± 50.3	89.2 ± 3.9	10.8 ± 3.8